



ELSEVIER

Available online at www.sciencedirect.com

SCIENCE @ DIRECT®

Journal of Crystal Growth ■■■■■ ■■■■■ ■■■■■

JOURNAL OF
**CRYSTAL
GROWTH**www.elsevier.com/locate/jcrysgr

Study of the morphology of copper hydroxynitrate nanoplatelets obtained by controlled double jet precipitation and urea hydrolysis

C. Henrist*, K. Traina, C. Hubert, G. Toussaint, A. Rulmont, R. Cloots

Laboratory of Inorganic Structural Chemistry (LCIS), General Chemistry Department, University of Liège, B6 Sart-Tilman, B-4000 Liège, Belgium

Received 1 January 2003; accepted 26 February 2003

Communicated by D.T.J. Hurlé

Abstract

A copper hydroxynitrate of stoichiometry $\text{Cu}_2(\text{OH})_3\text{NO}_3$, analogous to the layered double hydroxide family, was synthesized by the so-called controlled double jet precipitation technique, and by hydrolysis of urea in the presence of copper nitrate. Special attention has been focused on the size, morphology and agglomeration tendency of the particles. The aim of this work is to define the optimum precipitation conditions in terms of quality and dispersability of the recovered product. Such platelet-like particles can be used as anisotropic fillers in nanocomposite materials. Several reaction parameters such as flow and concentration of the reactant solutions, design of the reactor and addition of a growth modifier were studied.

© 2003 Published by Elsevier Science B.V.

Keywords: A1. Characterization; A1. Crystal morphology; A1. X-ray diffraction; A2. Growth from solutions; B1. Copper hydroxynitrate.

1. Introduction

Nanocomposite materials cover a very large variety of organic–inorganic hybrids. A nanocomposite is characterized by a high degree of dispersion of inorganic filler, to a nanoscopic level, in a polymer matrix. This can be done either by mixing them together at a temperature above the melting of the polymer, or by using an aqueous suspension of the inorganic filler in the case of

emulsion polymerization. Besides, many studies have been recently devoted to the development and characterization of new nanocomposites exhibiting anisotropic morphologies [1–7]. Specific mechanical and physical properties are expected when the filler particles are not spherical but elongated in one dimension (fibers) or two dimensions (platelets) [8,9]. The interest of composites containing nanoplatelets is mainly due to the improvement of their mechanical reinforcement properties as well as “barrier properties” that are supposed to play a significant role in fire resistance of such composites [10]. In this regard, efforts to control the morphology and agglomeration beha-

*Corresponding author. Tel.: +32-4-366-3438; fax: +32-4-366-3413.

E-mail address: catherine.henrist@ulg.ac.be (C. Henrist).

1 vior of inorganic copper hydroxynitrate nanoplatelets are of interest.

3 Moreover, while inorganic cation exchangers, including layered silicates or transition metal
5 oxysalts, are well represented in the literature, their anion exchangers counterparts have received
7 fewer attention [11]. As an example, copper (II) phenylphosphonate can be successfully obtained
9 by intercalation of the phosphonate ion, using the layered copper hydroxynitrate as the host material
11 [12]. The main current application of copper hydroxynitrate deals with its use as an oxidizer
13 in non-toxic, low-ash solid propellant and ignition compositions, especially for inflation of vehicle
15 airbags [13] that gave rise to several patents. On a morphology control point of view, the study of
17 inorganic chemistry of aqueous copper basic salts is of paramount importance in the scope of
19 coprecipitation methods for synthesizing precursors of copper-containing mixed oxide ceramics, in
21 particular, the superconducting phases [14,15].

23 We present in this paper some recent results about the influence of the precipitation conditions
25 on the morphology of Cu-layered double hydroxide (LDH)-type nanoplatelets obtained by controlled
27 double jet precipitation (CDJP) [16–20] and by hydrolysis of urea [21,22]. The dispersability of
29 the powders was also studied in aqueous suspension.

49 The $\text{Cu}_2(\text{OH})_3\text{NO}_3$ structure has been recently re-examined by Guillou et al. [23] and belongs to
51 the P2_1 space group with $z = 2$; the crystal system is monoclinic with $\beta = 94.619^\circ$ and the cell
53 parameters $a = 5.6005 \text{ \AA}$, $b = 6.0797 \text{ \AA}$, $c = 6.9317 \text{ \AA}$ at 25°C . The structure can be viewed
55 as layers of Cu octahedra stacked upon each other. Two types of copper octahedra exist: Cu(1) atoms
57 are coordinated by four OH^- groups and two oxygen atoms belonging to NO_3^- groups. The
59 Cu(2) atoms are coordinated by four hydroxyls, the fifth OH^- standing a bit further and an oxygen
61 atom belonging to a NO_3^- group. The copper octahedra form layers of stoichiometry
63 $[\text{Cu}_2(\text{OH})_3]^+$. Consequently, NO_3^- ions stand between the positive layers for charge balancing
65 and are linked by hydrogen bonding to the hydroxyl groups belonging to the copper octahedra
67 layers (Fig. 1). Due to its layered structure, $\text{Cu}_2(\text{OH})_3\text{NO}_3$ is expected to crystallize in platelet-
69 shaped particles.

71 While working on the preparation of uniform colloidal copper oxide by CDJP, Lee and Matijevic [24]
73 have observed that the stoichiometry as well as the morphology of the particles obtained by
75 reaction between NaOH and $\text{Cu}(\text{NO}_3)_2$ depend on the $[\text{NaOH}]/[\text{Cu}(\text{NO}_3)_2]$ molar ratio. For a
77 molar ratio comprised between 1.0 and 1.5, a copper hydroxynitrate $\text{Cu}_2(\text{OH})_3\text{NO}_3$ is precipitated
79 as hexagonal platelets. When this molar ratio

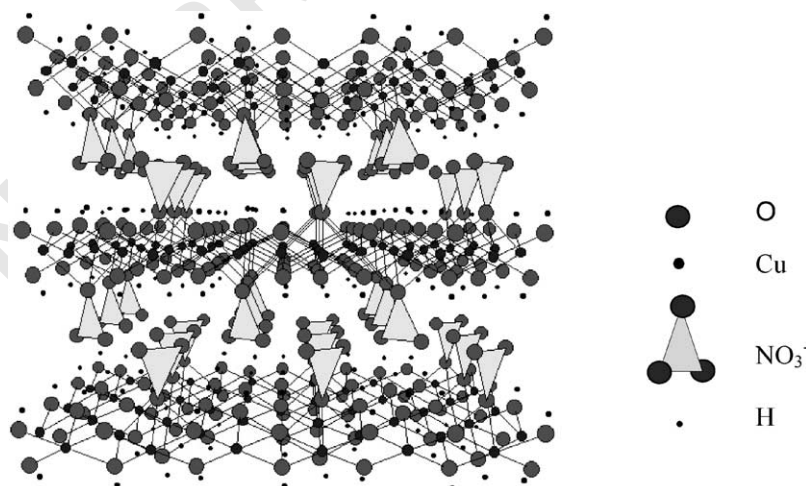


Fig. 1. Crystal structure of $\text{Cu}_2(\text{OH})_3\text{NO}_3$ showing the anchoring of nitrate groups in the layers of stoichiometry $[\text{Cu}_2(\text{OH})_3]^+$.

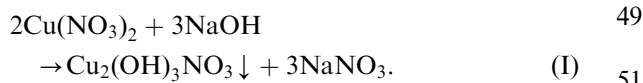
is increased above 1.5, CuO ellipsoids are formed and CuO needles appear if the ratio is increased further above 2.0. The temperature also plays a role in the morphology and chemical composition of the end-product: hexagonal platelets of copper hydroxynitrate do not form anymore at a temperature higher than 50°C. The main drawback of this technique is the very low concentration of solid in the suspension after complete addition of the reactant solutions—around 1 g/l. In order to improve the yield of this batch synthesis while keeping the desired size and morphology of the particles, we have tried to increase the concentration of the reactant solutions as well as their rate of addition into the reactor. Besides, a new continuous precipitation reactor has been designed in an attempt to bypass the problem of high dilution of the product. Finally, some trials have been made concerning the addition of growth modifiers that are expected to adsorb preferentially on certain crystal planes of the growing particles and therefore inhibit the growth in such direction, yielding more anisotropic particles.

Alternately to the precipitation technique, copper hydroxynitrate can be obtained by reacting copper nitrate and urea [21,22]. Urea will act as a reservoir for hydroxyl ions in solution, since these are released along the whole process by hydrolysis of urea upon heating. Krathovil et al. [21] have studied the influence of urea concentration and copper nitrate concentration onto the particles morphology obtained at 90°C after 2 h of maturation in solution. They have observed that platelet-like particles are not formed for every copper nitrate concentrations but are obtained in a narrow range of solution composition.

2. Experimental section

2.1. Double jet precipitation

The synthesis of $\text{Cu}_2(\text{OH})_3\text{NO}_3$ have been performed following the conditions described by Lee and Matijevic [24]: the reaction takes place between copper nitrate and sodium hydroxide (Eq. (I)):



Copper nitrate has to be maintained in excess in order to prevent the formation of copper hydroxide ($\text{Cu}(\text{OH})_2$) or copper oxide (CuO): the $[\text{OH}^-]/[\text{Cu}^{2+}]$ molar ratio is thus adjusted to 1. The final pH of the suspension is weakly acid, around pH 5. The “classical conditions” are the following: the reactant solutions are prepared by simple dissolution of the salts in de-ionized water. Copper salt solution and sodium hydroxide solution of concentration 0.1 M are simultaneously added to the reactor containing an initial water volume of 200 ml, with Heidolph peristaltic pumps working at a discharge of 10 ml/min. The total injection time is adjusted to 4 min. The suspension is let to mature during 5 days at a temperature of 25°C. The solid phase obtained after reaction is recovered by centrifugation at 4000 rpm and washed two times with water, then air-dried at 60°C overnight. Two types of reactors have been tested: the first one is a classical CDJP reactor and the second one has been designed in an attempt to reach a brutal dilution of the particles straight away after their formation in order to avoid growth and agglomeration (Fig. 2). This home-

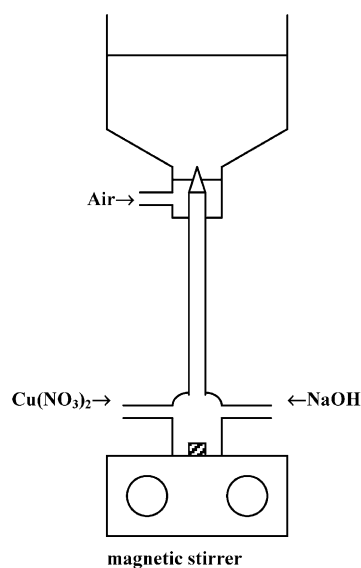


Fig. 2. “Diluting” CDJP reactor.

made “diluting” CDJP reactor is composed of three parts: the reactant solutions are injected into a small reaction chamber where they are vigorously stirred by a cruciform magnet. The resulting suspension then flows up through a pipe, into a dilution chamber containing a large volume of deionized water. Injection of air at this point allows a better dispersion of the particles in suspension.

2.2. Urea hydrolysis

Urea acts as the base reservoir. In aqueous solution, it decomposes upon heating into ammonia and HNCO following the equation given below:



In acidic or neutral conditions, HNCO is converted into carbon dioxide, and ammonia is converted into ammonium cation (Eqs. (III) and (IV)):



Reactions (III) and (IV) are proton consuming, thus promoting a progressive increase of the solution pH. The precipitation reaction being hydroxyl consuming, the urea hydrolysis equilibrium is displaced towards the end-products. Copper nitrate and urea solutions are placed in a beaker in a heating bath set at 90°C under moderate stirring. The solid phase that slowly appears is let to mature for 2 h in the mother liquor, then separated by centrifugation at 4000 rpm and washed with deionized water. Drying of the powder at 60°C is applied for one night. The concentrations have been chosen according to the results published by Krathovil et al. [21] and presented in Table 2.

2.3. Characterization techniques

The particles morphology is observed by scanning electron microscopy (SEM) on a Philips ESEM XL30 FEG microscope after coating of the sample by a thin, conductive gold layer obtained by sputtering under vacuum. The crystal-

linity of the end-product is checked by X-ray diffraction analysis (XRD) on a Siemens D5000 diffractometer working with Cu K α radiation and Ni filter. Particles size distribution in solution was measured with a Malvern Mastersizer Hydro2000S granulometer, while the mean size of the particles in the dry powder was determined by visual observation of SEM micrographs on a minimum of 100 particles. Infrared absorption spectra were obtained on a FT-IR spectrometer 1760X from Perkin Elmer. Around 1.5 mg of the sample was mixed with 800 mg of vacuum-dried KBr and pressed as pellets under a 1300 MPa pressure. A simultaneous thermal analysis was performed in a Netzsch apparatus, model STA 449C, in order to obtain the TG-DSC data. The powder was placed in an alumina crucible and heated under air at a rate of 10 K/min.

3. Results and discussion

3.1. Morphological aspects

3.1.1. Double jet precipitation

Several parameters have been studied: type of reactor (samples 1 and 2), flow of reactant solutions (samples 1, 3–7), concentration (samples 1 and 8) and addition of a growth modifier (samples 9 and 10). All synthesis conditions are summarized in Tables 1 and 2.

3.1.1.1. Type of reactor. The particles obtained by precipitation of Cu₂(OH)₃NO₃ in the two reactors presented above are characterized by relatively different morphologies, which are displayed in the SEM micrographs in Fig. 3. As can be seen in Fig. 3a, the diluting reactor leads to the tabular morphology, but the particles exhibit a peculiar arrangement typically resulting from intergrowth mechanism. It is clearly showed that the individual platelets are not simply randomly piled up, but have simultaneously grown from pre-agglomerated seeds and are therefore impossible to separate by any soft process. Vigorous grinding or hydrothermal post-treatment of the powder do not affect this particles morphology obtained at 60°C. In contrast to this, using the classical CDJP reactor

Table 1
Synthesis conditions of samples obtained by CDJP

Sample	Type of reactor ^a	Reactants solutions concentration (mol/l)	Discharge of reactants solutions (ml/min)	Additive
1	C	0.1	10	—
2	D	0.1	10	—
3	C	0.1	20	—
4	C	0.1	100	—
5	C	0.1	200	—
6	C	0.1	350	—
7	C	0.1	450	—
8	C	1.0	450	—
9	C	0.1	10	SDS
10	C	0.1	10	NaNO ₃

^aC: classical; D: diluting.

Table 2
Synthesis conditions of samples obtained by urea hydrolysis

Sample	[(NH ₂) ₂ CO] (mol/l)	[Cu(NO ₃) ₂] (mol/l)
11	0.1	0.03
12	0.2	0.06

produces well defined and separated tabular particles with elongated hexagonal, slightly indented contour. The mean dimensions of the particles were determined by image analysis based on SEM micrographs: the average length is 508 nm while the width was evaluated to be 316 nm (see Table 3). This difference can also be evidenced in the XRD pattern. It can be seen in Fig. 4 that sample 1 exhibits a higher I_{001}/I_{120} ratio than sample 2, which indicates a more pronounced orientation of the single platelets towards the incident X-ray radiation. This preferential orientation is not possible in the case of the tangled up arrangement of the particles.

We can explain these behaviors starting from observations during the reaction. At the first stage of the reaction, in the classical CDJP reactor, the suspension remains transparent and dark blue, revealing the presence of the six-fold coordinated cupric ion in solution. Later on, the suspension turns light blue and becomes turbid: the copper hydroxynitrate precipitates. On the other hand,

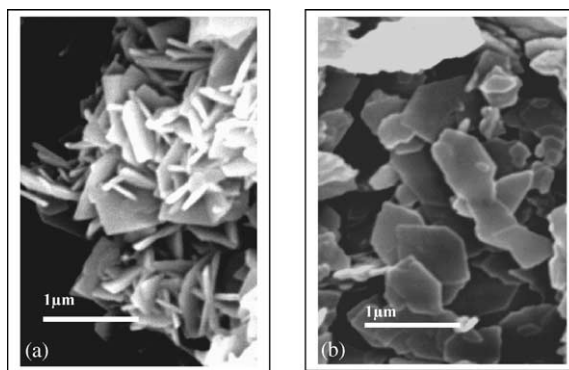


Fig. 3. SEM micrographs of Cu₂(OH)₃NO₃ particles synthesized: (a) in the “diluting” reactor (sample 2) and (b) in the classical reactor (sample 1).

Table 3
Mean particles size determined by image analysis based on SEM micrographs

Sample	Length (nm)	Width (nm)
1	508	316
8	246	153
10	408	226

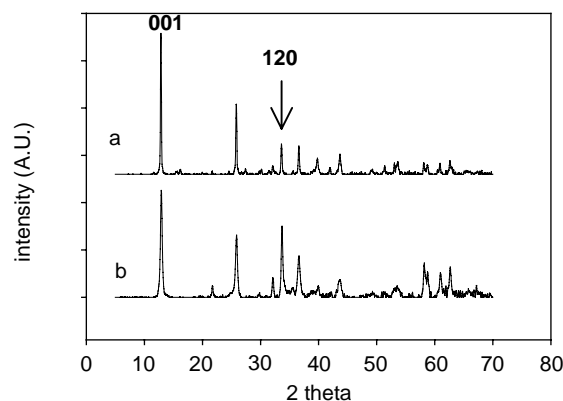


Fig. 4. XRD pattern of (a) sample 1, $I_{001}/I_{120} = 4.7$ and (b) sample 2, $I_{001}/I_{120} = 1.5$.

when working in the “diluting” reactor, we do not observe the transparent dark blue stage of the solution but straight away the turbid light blue suspension of solid. This is due to the high

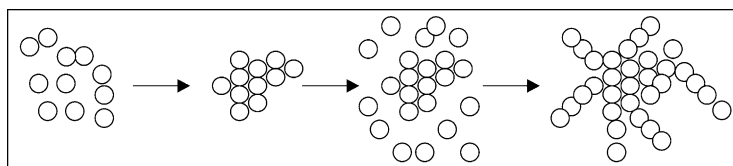


Fig. 5. Hypothetical growth mechanism proposed for the diluting CDJP reactor.

concentration of reactants present in the small reacting chamber: there is no water volume initially present in the reacting chamber before the addition of the reactants, and the critical concentration value (according to the LaMer model, see Ref. [25]) is therefore immediately reached. The high supersaturation conditions induce the formation of primary particles at the very beginning of the reaction. It is expected that these primary particles would quickly get agglomerated to lower their surface energy and form secondary particles, which flow up into the diluting chamber. At this stage, secondary nucleation and growth processes are running by classical bidimensional surface nucleation mechanism due to the low supersaturation conditions so obtained, as schematically illustrated in Fig. 5.

From these observations, we have decided to give up the diluting reactor for the following synthesis, expecting to avoid this agglomeration tendency that occurs when using this type of reactor.

3.1.1.2. Flow of reactants solutions. The quantity of recoverable product was kept constant: the time of injection was adjusted according to the flow of solution (values reported in Table 4) and trials were made at 25°C and 40°C. From SEM observations (not shown here), it came out that the discharge value of reactants solution into the reactor does not influence the morphology nor the agglomeration of the particles obtained, whatever be the temperature. The mean size and morphology of particles in samples 1, 3–7 were very similar to each other, around 500 nm in length and 305 nm in width. However, we have observed that increasing temperature promotes the precipitation of copper hydroxynitrate crystals with tabular morphology more quickly: from 5 days, at 25°C, to 1 h, at 40°C.

Table 4

Conditions of addition for the study of the influence of the flow at 25°C and 40°C

Flow (ml/min)	10	20	100	200	350	450
Time of injection (s)	240	120	24	12	7	5

3.1.1.3. Concentration. In order to increase the mass of recoverable solid product, the concentration of the reactant solutions have been increased ten times. The discharge of reactant addition has been fixed at 450 ml/min regarding the fact that this parameter does not seem to have a strong effect on the morphology and size of the obtained particles. Forty milliliters of 1 M reactant solutions was injected to the reactor containing 300 ml of water. The final solid concentration was 0.035 M. This solid was recovered after a 5-day maturation time at 25°C. As shown in Fig. 6, the resultant powder is constituted of small subunits of copper hydroxynitrate crystallites exhibiting a strong agglomeration behavior. The very high supersaturation conditions, immediately reached during the quick addition of the reactant solutions, have promoted a burst out of numerous, tiny nuclei in the initial mixture. According to the La Mer model [25], tridimensional nucleation proceeds so fast that the concentration of precursors in solution decreases rapidly, avoiding further nucleation and growth. Since the initial nuclei formed in a precipitation process are characterized by an isotropic geometry, it is therefore not surprising to observe that the particles obtained in these conditions have not reached a tabular morphology. Small particles have a tendency to agglomerate in solution in an attempt to decrease their surface energy, which seems to be the case here, since randomly branched strings of knitted sub-

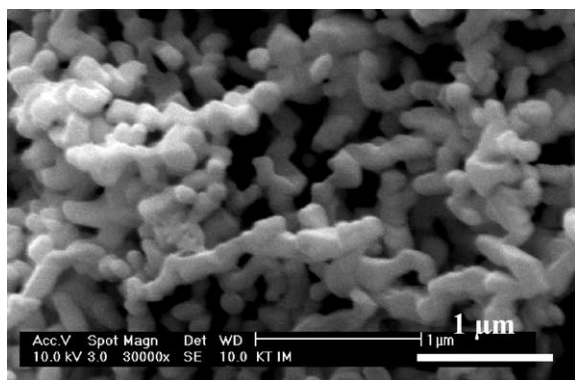


Fig. 6. SEM micrograph of particles formed in sample 8 after 5 days of maturation at 25°C. Scale: bar 1 μm.

units are observed in the micrograph presented in Fig. 6. However, this agglomeration appears to take place after complete formation of the crystallites, in opposition to the mechanism described for the “diluting” reactor (see above).

From these observations, it appears that the higher the concentration of reactants injected, the smaller the particles. Comparing the particles sizes of samples 8 and 10, determined by image analysis and presented in Table 3, shows that the particles obtained in concentrated conditions are twice as small as those obtained from the classical conditions.

3.1.1.4. Growth modifier and anti-agglomeration agent. Growth modifiers are used when one tries to promote or prevent crystal growth in one direction [18,19,26,27]. Their efficiency is based on preferential physical or chemical absorptions on selected surface sites present on the growing crystal faces. By this mean, precursors from the solution cannot reach the hindered growth sites anymore. In order to produce anisotropic crystallites, the affinity of the growth modifier towards the growth sites must be as different as possible for the different crystal faces. The amount of growth modifier molecules is also determined: if all the faces are blocked, no more growth will take place at all and tiny isotropic crystals will remain in suspension. Generally speaking, any ion or molecule able to interact with a surface site on the particle facets can be used as a growth modifier.

Surfactant molecules, literally meaning “surface active agents”, are commonly chosen due to their amphiphilic nature: the polar or ionic head group is anchored to the surface of the crystallite, while the non-polar hydrocarbon tail group points toward the solution, encapsulating the particle in a hindering layer. This steric effect is known to decrease the agglomeration level of particles in the suspension and in the resulting powder. Consequently, when properly chosen, a surfactant can play both roles: as a growth modifier and as an anti-agglomeration agent. A widely used surfactant is SDS, sodium dodecylsulfate, which consists of a 12-carbon chain with a sulfate functional head group. It was added in small quantity of the order of 5 wt% relative to the mass of copper hydroxynitrate, and introduced before the precipitation reaction takes place, either in the initial water volume present in the reactor (sample 9), in the NaOH solution or in the $\text{Cu}(\text{NO}_3)_2$ solution prior to injection. In all cases, similar results were observed: the mean size of the particles is slightly smaller than before (around 470 nm in length) but the morphology is kept identical. No decrease of the thickness of the particles can be proved. It is likely that the adsorption of the SDS molecules onto the particles facets was not selective but occurred randomly on all the faces.

The facets exhibited by a crystal are those characterized by a minimal surface free enthalpy. The crystal has two possibilities to decrease this term of enthalpy: either by exhibiting low Miller indexes faces or by adsorbing ions or molecules onto high Miller indexes faces. In the precipitation reaction, the counter-ions form sodium nitrate in solution. Moreover, in the classical conditions described before, the molar ratio $[\text{OH}^-]/[\text{Cu}^{2+}]$ is equal to unity, leading to an excess of copper nitrate in solution. One of these ions (Cu^{2+} , Na^+ or NO_3^-) probably adsorbs onto one face and promotes the formation of the tabular morphology. We drove the reaction in the reactor containing a sodium nitrate solution in place of the water volume usually present, then the suspension was allowed to age for 5 days at 25°C. The initial sodium nitrate solution concentration was adjusted to 0.05 M. A SEM micrograph of sample 10 is shown in Fig. 7. It is seen that the overall

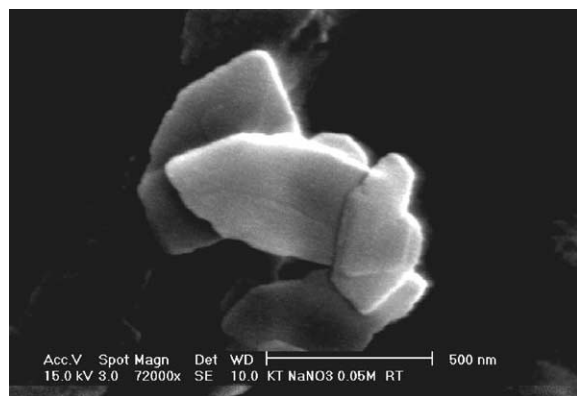


Fig. 7. SEM micrograph of particles formed in sample 10 after 5 days of maturation at 25°C. Scale: bar 500 nm.

geometry is kept identical: an elongated hexagonal contour with slight indentation. The mean particles size is however a 30% smaller than the samples obtained without sodium nitrate (see Table 3, samples 1 and 10). From this, it is thought that sodium and/or nitrate ions do not show a pronounced preferred adsorption on the basal plane of the crystallites rather than on the edges, since the edgewise growth appears to be a little bit slowed down. Other possible explanation would be related to the 0.05 M concentration that could exceed the saturated adsorption concentration corresponding to the basal planes.

3.1.2. Urea hydrolysis

The method based on urea hydrolysis leads to the obtention of crystals with remarkably improved morphology. Samples 11 and 12 gave similar results. Copper hydroxynitrate precipitates as very large, elongated hexagonal platelets with a sharp contour (Fig. 8). The particles seem also a bit thicker than their CDJP-precipitated counterparts. Their size was not accurately determined but SEM micrographs show that a 10 μm size is easily attained. Some intergrowth sites are visible in Fig. 8, probably arising from the low mechanical stirring and high-temperature conditions.

3.2. Molecular characterizations

Infrared spectroscopy and thermal analysis give access to additional molecular-scale information

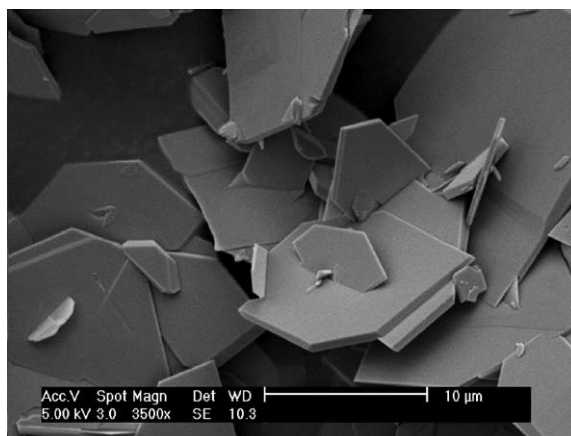


Fig. 8. SEM micrographs of particles in sample 11 after 2 h of urea hydrolysis at 90°C. Scale: bar 10 μm .

concerning the structure of the compound. At this level, both synthesis methods (CDJP and urea hydrolysis) show no difference neither in chemical purity nor in the proper crystal structure of the samples. Fig. 9 shows the FT-IR spectrum of a copper hydroxynitrate sample obtained by precipitation (the spectrum of a sample obtained by urea hydrolysis is identical). Secco and Worth [28] studied in detail the vibrational properties of this compound. IR absorptions are essentially due to hydroxyl and nitrate groups. Carbon dioxide is present as a contaminant with a specific peak at 2344 cm^{-1} .

3.3. Hydroxyl absorptions

The OH groups give absorptions in the range 3600–3200 cm^{-1} . The wideness of the band is related to the degree of hydrogen bonding with neighboring OH groups. Fig. 9 shows a complex band in this region, with a fine and intense peak at 3547 cm^{-1} , corresponding to a nearly single hydroxyl, while other wider bands centered at 3456 cm^{-1} indicate hydrogen-bonded OH groups. A precise study of the crystal unit cell allows distinguishing between the different types of OH groups [23]. The hydroxyls also present torsion vibrations in the range 255–292 cm^{-1} , but these values are out of reach of the spectrometer.

The Cu–O–H bonds give rise to bending absorptions at different frequencies, depending

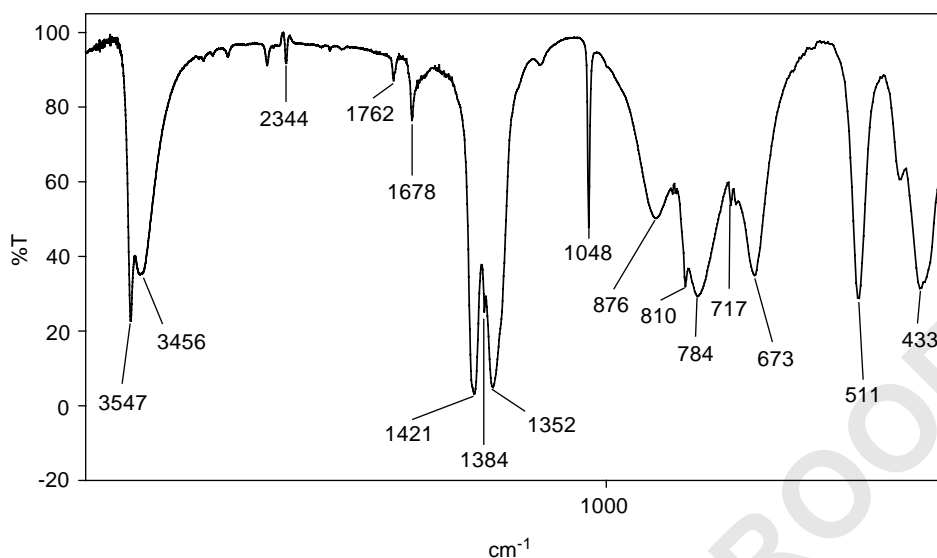


Fig. 9. Infrared spectrum of $\text{Cu}_2(\text{OH})_3\text{NO}_3$ (2 mg/800 mg KBr) from 400 to 4000 cm^{-1} .

Table 5
Infrared absorptions of nitrate groups

Frequency	ν_1 (cm^{-1})	ν_2 (cm^{-1})	ν_3 (cm^{-1})	ν_4 (cm^{-1})
Literature [23]	1040–1067	801–839	1313–1432	702–741
Experimental	1048	810	1352–1384–1421	?–717
	Intense and fine	singlet	multiplet	Doublet of equal intensity

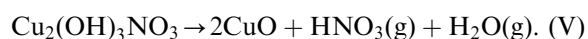
on the degree of hydrogen bonding: 878, 780, 675 cm^{-1} . Experimentally, we observe absorption bands located at 876, 784 and 673 cm^{-1} .

3.4. Nitrate absorptions

While the isolated nitrate ion gives only two active vibration modes in infrared (ν_2 and ν_4), the nitrate ion anchored in the crystal absorbs the infrared radiation at the four frequencies corresponding to ν_1 , ν_2 , ν_3 and ν_4 . Harmonics and combination peaks rend the spectrum still more complex. Assignations of nitrate vibrations are summarized in Table 5.

Thermal analysis of the copper hydroxynitrate shows its thermal decomposition and subsequent conversion into copper oxide [22]. Although this decomposition takes place in one single step, it follows the mechanism described by the following

equation:



This decomposition mechanism does not imply the dissociation of gaseous nitric acid, as it is currently admitted. Auffrédic et al. [22] have shown that, if the dissociation of HNO_3 to give H_2O , NO_2 (g) and O_2 (g) is thermodynamically favoured, the decomposition kinetics is extremely slow below a temperature of 150°C, and becomes significant only starting from 250°C. However, as Fig. 10 shows, the main mass loss is accomplished at this temperature. The TG curve attests a single-step degradation that is accompanied by an endothermic effect related to the evolved gaseous components. The total mass loss reaches 34.7 wt% at 500°C, which is in good agreement with the theoretical value of 32 wt% [24].

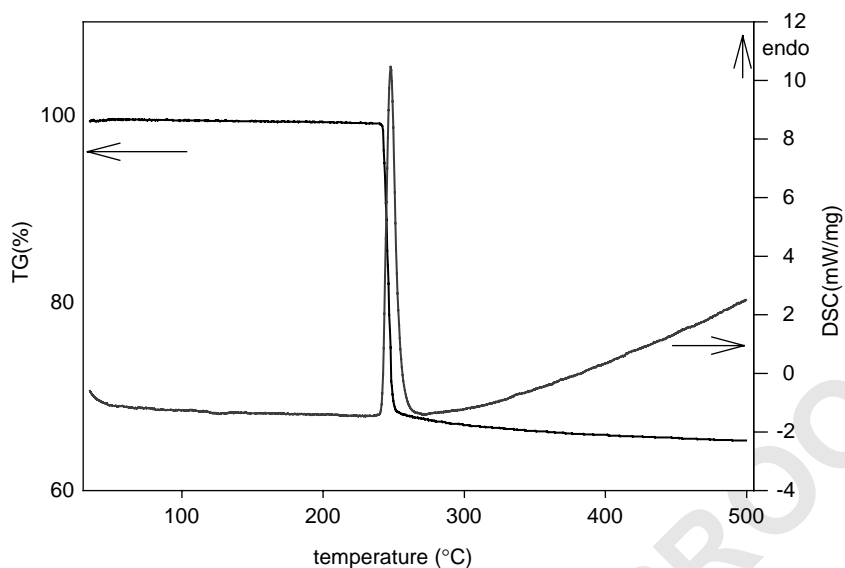


Fig. 10. Thermal analysis of copper hydroxynitrate: TG and DSC curves from RT to 500°C under air. Heating rate = 10 K/min.

3.5. Dispersability

Aqueous slurries can be used to incorporate the inorganic filler in a water-soluble polymer, or can even be added during the synthesis of an emulsion-driven polymerization of PVC, for example. In this respect, it is interesting to control the stability of the suspension and avoid the formation of large agglomerates of particles in water, prior to the mixing with the polymer. Fig. 11—dashed curve shows the size distribution in volume of the copper hydroxynitrate powder corresponding to sample 1, without any dispersing aid other than stirring. It shows that the platelets tend to aggregate in water to form big clusters of mean size ca. 15 μm . A dispersant additive was used in order to improve the dispersion of the particles in suspension: *Dispex N40V*, a sodium polyacrylate in aqueous solution. Five drops of *Dispex N40V* solution (0.1445 g) were added to the tank containing 10 ml of mother solution and 110 ml of water. Stirring and ultrasonication was applied during 15 min before making the granulometric measurement (see Fig. 11—solid curve). The distribution curve shows an important maximum at ca. 0.194 μm , which can be assigned to single platelets in

suspension. Increasing the *Dispex N40V* concentration does not improve the dispersion effect. It is therefore proposed that *Dispex N40V* acts rather as a stabilizer of particles previously mechanically separated by the ultrasonic bath. On the other hand, the particles dispersion cannot be performed only by ultrasonic exposure. It is important to stress that the best dispersion effect is obtained by using the two techniques simultaneously.

4. Conclusions

From the results that have been described above, some guidelines can be proposed concerning the production of copper hydroxynitrate by a precipitation reaction starting from sodium hydroxide and copper nitrate solutions. The flow of injection into the CDJP reactor does not affect the size nor the morphology of the particles, at 25°C as well as at 40°C. Experiments related to the concentration of the reactant solutions have shown that the size of the particles depends strongly on the molal concentration of the precipitate. The increase of this concentration is accompanied by a decrease of the mean size of the

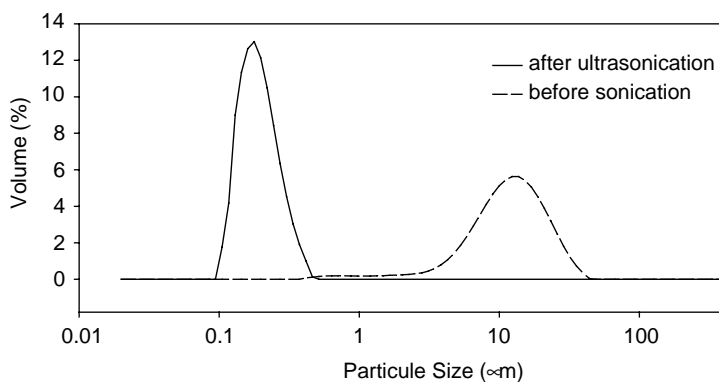


Fig. 11. Distribution in percent volume of the particles in sample 1 in aqueous suspension: (---) as-synthesized slurry; (—) slurry after ultrasonication in the presence of a dispersant. For experimental details, see the text.

particles and a loss of tabular morphology. The use of sodium nitrate as an adsorbent allowed us to produce slightly smaller particles at 25°C. The optimum conditions to produce thin, non-agglomerated particles in a short ageing time are thus encountered when working in a classical CDJP reactor, with a low concentration of sodium nitrate added in the water volume initially present in the reactor, and allowing the suspension to age at 40°C for 1 h.

On the other hand, working with the urea as a source of hydroxyl ions allows a slow and better-controlled formation of the precipitate. The striking difference lies in the size and morphology of the particles, which are 20 times larger and have a better-defined geometry. However, this great increase in size is accompanied by an increase in thickness that may be incompatible with nanofiller applications.

Finally, good dispersion of the powders in aqueous suspension was obtained by performing ultrasonication on the solution containing small quantities of a commercially available anionic dispersant, Dispex N40V.

Acknowledgements

The authors acknowledge Dr. C. Vogels, SOLVAY S.A., for financial support and valuable scientific discussions.

References

- [1] J.E. Gardolinski, L.C.M. Carrera, M.P. Cantao, F. Wypych, *J. Mater. Sci.* 35 (2000) 3113.
- [2] V. Mehrotra, E. Giannelis, *Solid State Commun.* 77 (1991) 155.
- [3] P.B. Messersmith, E.P. Giannelis, *Chem. Mater.* 6 (1994) 1719.
- [4] R.A. Vaia, S. Vasudevan, W. Krawiec, L.G. Scanlon, E.P. Giannelis, *Adv. Mater.* 7 (1995) 154.
- [5] M. Alexandre, G. Beyer, C. Henrist, R. Cloots, A. Rulmont, R. Jérôme, Ph. Dubois, *Chem. Mater.* 13 (2001) 3830.
- [6] M. Alexandre, G. Beyer, C. Henrist, R. Cloots, A. Rulmont, R. Jérôme, Ph. Dubois *Macromol. Rapid Commun.* 22 (2001) 643.
- [7] D.M. Lincoln, R.A. Vaia, Z.G. Wang, B.S. Hsiao, *Polymer* 42 (4) (2001) 1621.
- [8] R. Krishnamoorti, K. Yurekli, *Curr. Opin. Colloid Interface Sci.* 6 (5-6) (2001) 464.
- [9] M.J. Solomon, A.S. Almusallam, K.F. Seefeldt, A. Somwangthanaroj, P. Varadan, *Macromolecules* 34 (6) (2001) 1864.
- [10] M. Alexandre, G. Beyer, C. Henrist, R. Cloots, A. Rulmont, R. Jérôme, Ph. Dubois *Macromol. Rapid Commun.* 22 (2001) 643.
- [11] C.S. Bruschini, M.J. Hudson, in: T. JPinnavaia, M.F. Thorpe (Eds.), *Access in Nanoporous Materials*, Plenum Press, New York, 1995.
- [12] H. Hayashi, M.J. Hudson, *J. Mater. Chem.* 5 (1) (1995) 115.
- [13] H. Schmid, N. Eisenreich, *Propellants, Explosives, Pyrotech.* 25 (5) (2000) 230.
- [14] F. Mahloojchi, F.R. Sale, N.J. Shah, J.W. Ross, *Br. Ceram. Proc.* 40 (1988) 1.
- [15] R.J. Candal, A.E. Regazzoni, M.A. Blesa, *J. Mater. Chem.* 2 (6) (1992) 657.

- 1 [16] J. Stavek, M. Sipek, I. Hirasawa, K. Toyokura, Chem. Mater. 4 (1992) 545.
- 3 [17] S.H. Lee, Y.S. Her, E. Matijevic, J. Colloid Interface Sci. 186 (1997) 193.
- 5 [18] Q. Zhong, E. Matijevic, J. Mater. Chem. 6 (3) (1996) 443.
- 7 [19] C. Goia, E. Matijevic, J. Colloid Interface Sci. 206 (1998) 583.
- 9 [20] Y.S. Her, E. Matijevic, M.C. Chon, J. Mater. Res. 10 (12) (1995) 3106.
- 11 [21] S. Kratochvil, E. Matijevic, J. Mater. Res. 6 (4) (1991) 766.
- [22] J.P. Auffrédic, D. Loüer, M. Loüer, J. Thermal Anal. 16 (1979) 329.
- [23] N. Guillou, M. Louer, D. Louer, J. Solid State Chem. 109 (1994) 307.
- [24] S.H. Lee, Y.S. Her, E. Matijevic, J. Colloid Interface Sci. 186 (1997) 193.
- [25] V.K. LaMer, R.H. Dinegar, J. Am. Chem. Soc. 72 (11) (1950) 4847.
- [26] A. Chittofrati, E. Matijevic, Colloids Surfaces 48 (1990) 65.
- [27] R.J. Candal, A.E. Regazzoni, M.A. Blesa, J. Mater. Chem. 2 (6) (1992) 657.
- [28] E.A. Secco, G.G. Worth, Can. J. Chem. 65 (1987) 2504.

UNCORRECTED PROOF